Supplementary Material: 2-hydroxy-1-naphthaldehyde (2H1N)

S1. S_0 geometry of 2H1N (*ab initio* calculations)

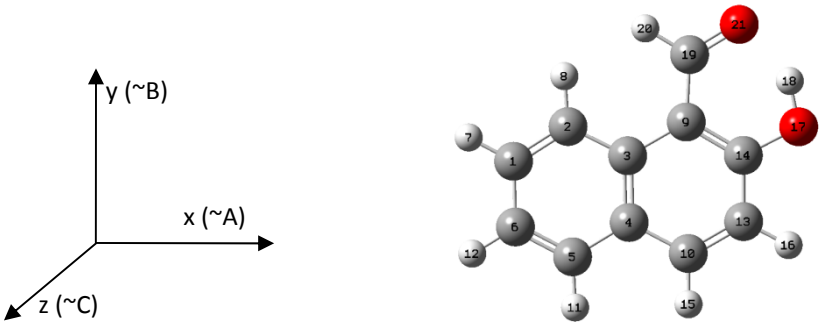

Figure S1: Gaussian calculation co-ordinate scheme. The orientations of the axes A, B, C (corresponding to the principle moments of inertia I_A, I_B, I_C) are also shown. The *z* co-ordinate corresponds exactly with C. The *y* and *x* axes correspond approximately (~ 99% correspondence) with B and A, respectively.

Table S1: DFT B3LYP/6-31G** optimised S_0 geometry of 2H1N.

Atom	*x*	*y*	*z*
C_1	0.000000	0.000000	0.000000
C_2	1.381346	0.000000	0.000000
C_3	2.116733	1.213028	0.000000
C_4	1.373254	2.435985	0.000000
C_5	-0.04253	2.405012	0.000000
C_6	-0.72571	1.208419	0.000000
H_7	-0.53239	-0.94667	0.000000
H_8	1.897653	-0.95292	0.000000
C_9	3.562153	1.278857	0.000000
C_{10}	2.076907	3.677427	0.000000
H_{11}	-0.58213	3.348504	0.000000
H_{12}	-1.81096	1.192781	0.000000
C_{13}	3.442794	3.737953	0.000000
C_{14}	4.203413	2.538088	0.000000
H_{15}	1.49668	4.596674	0.000000
H_{16}	3.979369	4.680236	0.000000
O_{17}	5.529289	2.659272	0.000000
H_{18}	5.898094	1.729123	0.000000
C_{19}	4.400471	0.099672	0.000000
H_{20}	3.906048	-0.88446	-0.000177
O_{21}	5.642854	0.12616	-0.000182

S2. Ground State Vibrational Frequencies

Table S2 lists the DFT B3LYP 6-31G** ground state vibrational frequencies of the optimised ground state geometry of 2H1N. All frequencies have been scaled by the recommended scale factor of 0.9611.[54] As 2H1N is an isomer of 1H2N, it exhibits the same number and type of vibrational modes as 1H2N, i.e. 39 modes of A' symmetry and 18 modes of A" symmetry. In-plane modes (A' symmetry) are denoted by $\nu'_{\#}$, where # is the number assigned to the mode. Out-of-plane (A" symmetry) modes are denoted by $\nu''_{\#}$. The modes are numbered in order of increasing frequency.

Table S2: Vibrational frequencies (DFT B3LYP/6-31G**) of the ground state (S_0) of 2H1N.The abbreviation naph.refers to the naphthalene rings of the 2H1N molecule i.e. the rings formed by the atoms $C_1 - C_6$ (inclusive) and C_9, C_{10}, C_{13} and C_{14}. Vibrations modulating the $O_{21}...H_{18}$ distance are described accordingly.

Totally symmetric (A') modes: S_0 (DFT B3LYP/6-31G)**			
Mode	**ν' [cm^{-1}]**	**$\nu'_{scaled} = 0.9611\upsilon$ [cm^{-1}]**	**Description**
ν'_5	252	242	Naph. ring C-C angle bends; CHO wag; strongly modulates $O_{21}..H_{18}$
ν'_7	352	338	Naph. ring C-C angle bends; OH wag; strongly modulates $O_{21}..H_{18}$
ν'_9	433	416	Naph. ring C-C angle bends
ν'_{10}	441	424	Naph. ring C-C angle bends (symmetric naph. ring stretching)
ν'_{11}	492	473	Naph. ring C-C angle bends; C=O bend; OH wag; strongly modulates $O_{21}..H_{18}$
ν'_{13}	543	522	Naph. ring C-C angle bends; modulates $O_{21}..H_{18}$
ν'_{15}	669	643	Naph. ring C-C angle bends (ring stretching); modulates $O_{21}..H_{18}$
ν'_{17}	733	704	C-C bond stretching; CH wags; O_{17}-H_{18} wag; modulates $O_{21}..H_{18}$.
ν'_{20}	782	751	Naph. ring C-C angle bends; modulates $O_{21}..H_{18}$
ν'_{22}	875	841	Naph. ring C-C angle bends
ν'_{27}	992	953	Naph. ring C-C angle bends; modulates $O_{21}..H_{18}$
ν'_{30}	1066	1025	Naph. ring breathing
ν'_{31}	1110	1067	C-H wags; C-C angle bends; modulates $O_{21}..H_{18}$
ν'_{32}	1173	1127	C-H wags
ν'_{33}	1195	1149	C-H wags
ν'_{34}	1209	1162	C-C bond stretching; CH wags; O_{17}-H_{18} wag; modulates $O_{21}..H_{18}$
ν'_{35}	1246	1197	"
ν'_{36}	1283	1233	"

ν'_{37}	1332	1280	"
ν'_{38}	1361	1308	"
ν'_{39}	1395	1341	"
ν'_{40}	1410	1355	"
ν'_{41}	1444	1388	"
ν'_{42}	1477	1420	"
ν'_{43}	1483	1425	"
ν'_{44}	1523	1464	"
ν'_{45}	1572	1510	"
ν'_{46}	1639	1575	"
ν'_{47}	1653	1589	"
ν'_{48}	1674	1609	"
ν'_{49}	1707	1641	C=O (i.e. C_{19}=O_{21}) bond stretching; modulates O_{21}..H_{18}.
ν'_{50}	3024	2906	C $_{19}$-H_{20} stretch (aldehyde group)
ν'_{51}	3144	3022	OH stretch; strongly modulates O_{21}..H_{18}.
ν'_{52}	3178	3054	CH stretches (naphthalene ring)
ν'_{53}	3183	3059	"
ν'_{54}	3189	3065	"
ν'_{55}	3207	3082	"
ν'_{56}	3217	3092	"
ν'_{57}	3221	3096	"

Non-totally symmetric (A'') modes: S_0 (DFT B3LYP / 6-31G **)			
Mode	**ν'' [cm^{-1}]**	**$\nu''_{scaled} = 0.9611\upsilon$ [cm^{-1}]**	**Description (Out-of-plane motion dominated by …..)**
ν''_1	85	82	All atoms. Moderate CHO and OH motion.
ν''_2	119	114	All atoms. Moderate CHO and OH motion.
ν''_3	203	195	All atoms. Moderate CHO and OH motion.
ν''_4	233	224	All atoms; Strong H_{20} and C_{19} motion (aldehyde group)
ν''_6	331	318	All atoms. Moderate CHO and OH motion.
ν''_8	414	398	All H and C atoms. Small CHO and OH motion.
ν''_{12}	507	487	All H and C atoms. Small CHO and OH motion.
ν''_{14}	551	530	Some H and C atoms. (Not CHO or OH)
ν''_{16}	686	659	All H and C atoms. Small CHO and OH motion.
ν''_{18}	763	733	Hydrogens (H_7, H_8, H_{11}, H_{12}, H_{15}, H_{16})
ν''_{19}	775	745	All H and C atoms. (Not CHO or OH)
ν''_{21}	843	810	Hydrogens (H_7, H_8, H_{11}, H_{12}, H_{15}, H_{16})
ν''_{23}	877	843	Hydrogens (H_7, H_8, H_{11}, H_{12}); Small H_{18} motion.
ν''_{24}	920	884	H_{18} (hydroxyl group)
ν''_{25}	952	915	Hydrogens (H_7, H_8, H_{11}, H_{12}, H_{15}, H_{16})
ν''_{26}	985	947	Hydrogens (H_7, H_8, H_{11}, H_{12}, H_{15}, H_{16})
ν''_{28}	992	953	Hydrogens (H_7, H_8, H_{11}, H_{12}, H_{15}, H_{16}, H_{20})
ν''_{29}	1008	969	H_{20} and C_{19} (i.e. CH of aldehyde group)

S3. Molecular Orbitals of 2H1N

The $S_1 \leftarrow S_0$ electronic transition of 2H1N comprises components of two molecular orbital (MO) transitions. It is predominantly composed of the MO 45 → MO 46 transition and also contains some MO 44 → MO 48 character. The Gaussian 03 representation of the DFT B3LYP/6-31G** calculation of these orbitals is shown in Fig. S2. Changes in the acidity and basicity of functional groups connected by an IMHB may drive a proton transfer process.[21,31,32,55] Referring to Fig. S2, acidity-basicity changes can be seen to occur in 2H1N upon excitation. A slight decrease in electron density in the region of the hydroxyl oxygen occurs for the MO 45 → MO 46 transition, indicating an increase in acidity of the hydroxyl oxygen. In addition the shrinkage of this bonding orbital indicates a weakening of the O_{17} – H_{18} bond upon excitation. Electron density surrounding the carbonyl oxygen remains virtually unchanged during the MO 45 → MO 46 transition. The MO 44 → MO 48 transition is accompanied by an increased concentration of the electron density centred on the carbonyl oxygen, indicating an increased basicity in this region.

In Part 1[13] it was noted that the changes in acidity and basicity of the aldehyde and hydroxyl groups of 1H2N, which occur upon excitation, are quite modest in comparison to those of some other known proton transfer molecules, e.g. MHN23.[14] Referring to Fig. S2, it can be seen that the alterations in acidity and basicity of 2H1N which occur upon excitation are similarly modest in comparison to MHN23.

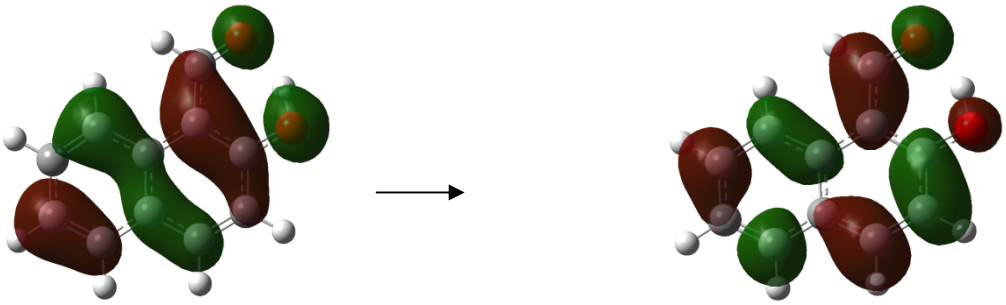

MO 45 (HOMO) **MO 46 (LUMO)**

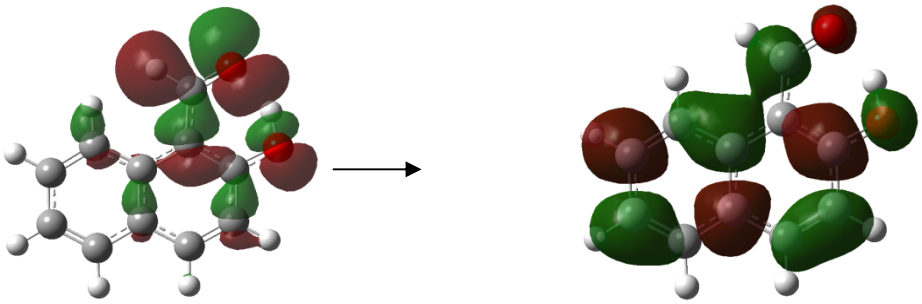

MO 44 **MO 48**

Figure S2: Molecular orbitals involved in the $S_1 \leftarrow S_0$ electronic transition of 2H1N.

S4. Excited Singlet States

The CIS 6-31G+ energies and oscillator strengths of the first four singlets of 2H1N were computed. In Table S3 the calculated values are compared with the absorption maxima of the solution spectrum of 2H1N in methyl cyclohexane.[22] The absolute error in the CIS calculation of the singlet energies is large (~10000 cm^{-1}). However, as with 1H2N[13] the CIS singlet energies appear to bear a qualitative resemblance to the experimentally measured absorption maxima.

The energy difference between the two experimentally measured absorption maxima is 3592 cm^{-1}. This appears to correlate with the theoretically calculated energy difference between S_1 and S_3 (4527 cm^{-1}) and the experimental maximum at 31447 cm^{-1} is tentatively assigned as S_3.

The second singlet S_2 is computed to lie close in energy to S_1 (2783 cm^{-1}) and has a very low oscillator strength ($f \sim 0.0004$). Hence, the S_2 singlet is likely to be obscured by the S_1 singlet in solution. The low oscillator strength of S_2 implies that it is likely to exhibit A" symmetry and is virtually impossible to observe.

Table S3: Gaussian calculation of singlet energies and oscillator strengths of 2H1N and the measured absorption maxima of 2H1N in cyclohexane solution.[22]

	CIS 6-31G +		Experimental[22]	
	Energy [cm^{-1}]	Osc. Strength, *f*	Abs max. [cm^{-1}]	Molar Ext. Coeff. (ε), [M^{-1} cm^{-1}]
S_1	36006	0.2808	27855	8000
S_2	38790	0.0004		
S_3	40534	0.1573	31447	12000
S_4	45733	0.0449		
$\Delta S_1..S_2$	2783			
$\Delta S_1..S_3$	4527		3592	
$\Delta S_1..S_4$	9727			

S5. Excited state geometry

The energies of the first four excited singlet states of 2H1N were calculated at CIS 6-31G+ level (see Table S3). Starting from the optimised ground state B3LYP 6-31G** geometry, a geometry optimisation and frequency calculation on S_1 of 2H1N was performed using the CI singles method (CIS) and the 6-31G basis set (geometry optimizations at the CIS 6-31G** and CIS 6-31G+ levels could not be performed due to computational limitations). The computed vibrational frequencies contained one imaginary frequency (indicated by a negative value) with an energy of (hc)×–66 cm^{-1}. The presence of one imaginary frequency indicates that the computed structure of S_1 is a first order saddle point, i.e. an energy maximum in one direction on the potential surface and an energy minimum in all other directions.[33] The computed structure is therefore not the lowest energy S_1 geometry but rather a 'transition' structure between two other S_1 energy minima.[#] The nature of the imaginary frequency of a first order saddle point can assist in determining the normal co-ordinate for which the saddle point is an energy maximum. Locating this normal co-ordinate indicates the geometry perturbation required to produce the true energy minima, on the potential surface. The –66 cm^{-1} vibration is an out-of-plane molecular vibration, which suggests that the computed

[#] A CIS 6-31G calculation was also carried out using the B3LYP 6-31G optimised ground state co-ordinates. However, this also produced a first order saddle point with the imaginary frequency – 66 cm^{-1}. Unsuccessful attempts were also made to locate the fully optimised excited state structure from a perturbed ground state structure. It may be possible to locate the fully optimised geometry of S_1 (i.e. the global energy minimum) by performing a full or partial potential energy surface scan. Alternatively, a TDDFT calculation of the excited S_1 state or a CIS calculation with a larger basis set may assist in locating the global minimum. These computationally costly calculations were not performed.

'transition' structure links two out-of-plane geometries which are energy minima on the S_1 potential energy surface. It is likely that one of these structures is the global minimum on the S_1 potential energy surface. It was hence concluded, that the S_1 geometry is likely to be an out-of-plane geometry. In contrast, the B3LYP 6-31G S_0 geometry was found to be exactly planar and the B3LYP 6-31G** S_0 geometry approximately planar.

S6. Gaussian fit of rovibronic envelopes in the $S_1 \leftarrow S_0$ fluorescence excitation spectrum of 2H1N

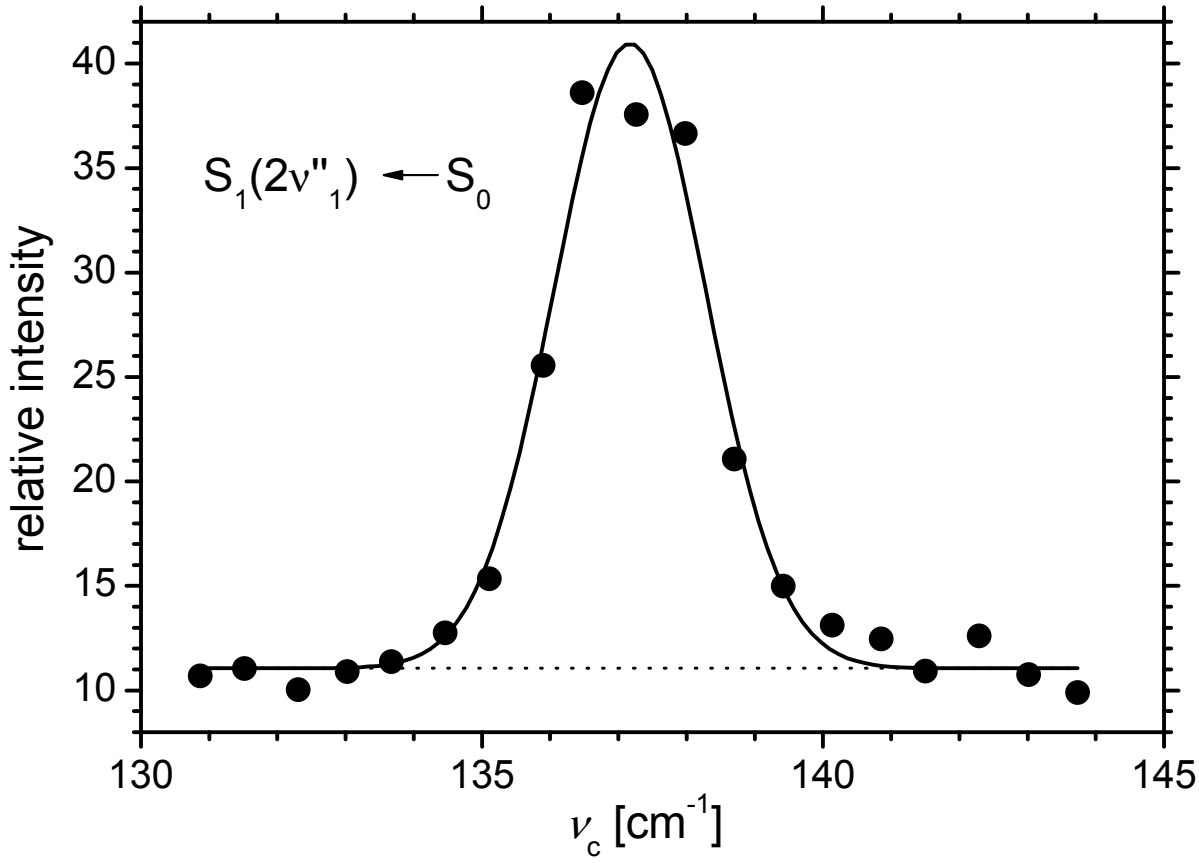

Figure S3: Gaussian fit to rovibronic envelope of line $S_1(2\nu''_1)$ of 2H1N. (●) Experimental points; (—) Gaussian Fit; (- - -) Baseline (I_0). Parameters: $\nu_c = 137.17$ cm^{-1}, $I_0 = 11.1$(arb. uits), $A = 83$ (arb. units), $\Delta\nu = 3.1$ cm^{-1}, $R^2 = 0.973$.

Table S4: Parameter list of Gaussian profiles

$$I(\nu) = I_0 + \frac{A}{w\sqrt{\pi/2}} \exp\left(-2\frac{(\nu-\nu_c)^2}{w^2}\right)$$

fitted to six vibronic lines of 2H1N. A is the area under the envelope, I_0 is the baseline, ν_c is the centre wavenumber, and $\Delta\nu = w\ (\ln 4)^{-0.5}$ is the full width at half maximum. The errors of $\Delta\nu$, I_0, ν_c and A are the standard errors calculated in the fitting procedure. The error of the average $\Delta\nu$ value, is the standard deviation of the $\Delta\nu$ values.

Excess Energy, ν_c [cm^{-1}]	assign.	$\Delta\nu$ [cm^{-1}]	I_0 [arb. units]	A [arb. units]	R^2
137.17 ±0.05	$2\nu''_1$	3.1 ± 0.1	11.1 ± 0.5	83 ± 4	0.973
156.50 ± 0.09	ν''_3	3.4 ± 0.2	10.9 ± 0.3	41 ± 3	0.935
245.80 ± 0.08	ν'_5	3.3 ± 0.2	12.0 ± 1.0	101 ± 9	0.942
357.67 ± 0.06	$\nu''_2 + \nu''_4$	2.2 ± 0.2	14.4 ± 0.4	28 ± 3	0.954
487.69 ± 0.08	ν'_{11}	2.5 ± 0.2	15.4 ± 0.8	39 ± 5	0.927
752.24 ± 0.07	ν'_{20}	2.8 ± 0.2	11.9 ± 0.3	35 ± 3	0.942
Average $\Delta\nu$ [cm^{-1}]:		**2.9 ± 0.5**			
Average R^2:					**0.9455**

S7. Temperature and pressure dependence of line intensity ratios in the $S_1 \leftarrow S_0$ fluorescence excitation spectrum of 2H1N

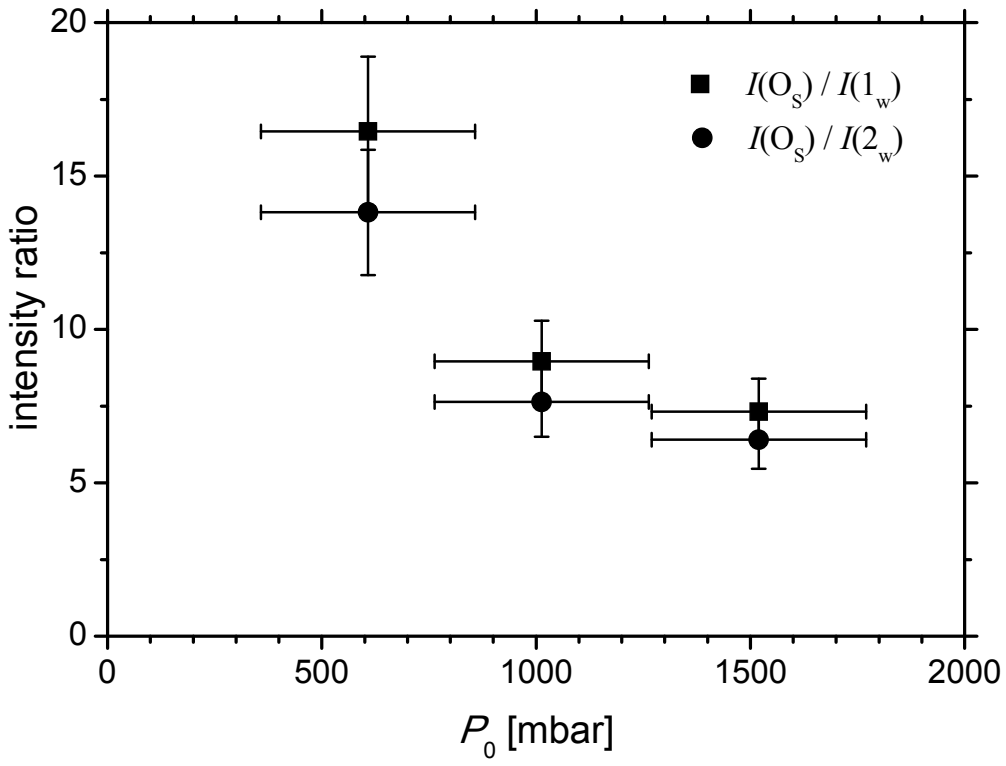

Figure S4: $[I(O_s)/I(1_w)]$ (■) and $[I(O_s)/I(2_w)]$ (•) as a function of backing pressure, P_0. $I(O_s)$, $I(1_w)$ and $I(2_w)$ are the intensities of the 'strong' origin at 26668 cm^{-1}, the line 1_w at 26578 cm^{-1} and the line 2_w at 26616 cm^{-1}, respectively. The errors in average intensity ratios is based on the standard deviation of the measured relative intensities. The estimated error in measured pressure values is ±250 mbar.

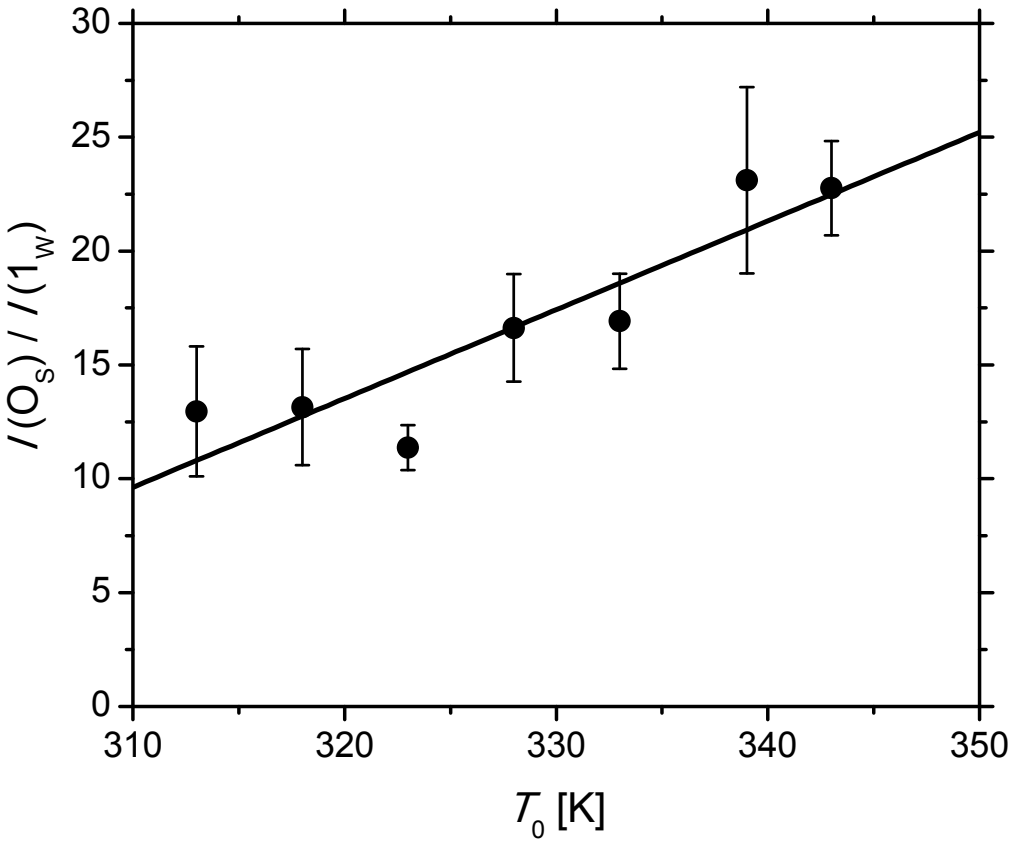

Figure S5: Plot of the ratio $[I(O_s)/I(1_w)]$ versus the temperature of the reservoir gas mixture, T_0. $I(O_s)$ and $I(1_w)$ are the intensities of the strong origin line, O_s (26668 cm^{-1}) and the feature 1_w (26578 cm^{-1}), respectively. The errors in the average relative intensities equate to the standard deviation of the measured relative intensities. The error in measured temperature values derives primarily from the positioning of the thermocouple with respect to the gas reservoir. This error is expected to be approximately uniform for the measured temperature range and is thus neglected here. The parameters of the linear regression ($[I(O_s)/I(1_w)] = A + BT$) are: $A = -110 \pm 30$, $B = (0.39 \pm 0.08)\ K^{-1}$, $R^2 = 0.787$.

References

13. A. McCarthy and A. A. Ruth, *Phys. Chem. Chem. Phys.*, **2011**, 13, 7485–7499 (part1).
14. A. McCarthy and A. A. Ruth, *Phys. Chem. Chem. Phys.*, **2011** (part 3), to be submitted.
22. P. Chowdhury, S. Panja and S. Chakravorti, *J. Phys. Chem. A*, **2003**, 107, 83–90.
30. R. B. Singh, S. Mahanta, S. Kar and N. Guchhait, *Chem. Phys.*, 2007, **331**, 373–384.
33. J. B. Foresman and A. Frisch, in *Exploring Chemistry with Electronic Structure Methods*, Gaussian, Inc., 2nd edn., 1996, p. 213.
53. S. Tobita, M. Yamamoto, N. Kurahayashi, R. Tsukagoshi, Y. Nakamura and H. Shizuka, *J. Phys. Chem. A*, 1998, **102**, 5206–5214.

54. K. Irikura, R. Johnson and R. Kacker, *J. Phys. Chem A*, **2005**, 109, 8430–8437
55. J Catalan, Journ. Of Amer. Chem. Soc, 2001, 123, 11940–11944.